

ORIGINAL ARTICLE

Sensing Properties of ZnO-SWCNT Hybrid Nanostructure Coated on Flexible Substrate for CO₂ Gas Detection

Aisyah Nur Estri^{1,*}, Riyani Tri Yulianti², Qonitatul Hidayah¹, Surip Kartolo³ and Rike Yudianti^{2,*}¹Faculty of Applied Science and Technology, University Ahmad Dahlan, Indonesia²Research Center for Advanced Material, National Research and Innovation Agency (BRIN), Indonesia³Research Center for Photonic, National Research and Innovation Agency (BRIN), Indonesia

ABSTRACT – We report sensing properties of functionalized single walled carbon nanotubes (f-SWCNTs) deposited on the flexible substrate of silicon (Si) and polyethylene terephthalate (PET). Deposition of f-SWCNT on Si rubber and PET surface was conducted by applying different manner of spray coating and dip coating techniques, respectively. Surface modification of f-SWCNT by ZnO nanostructure was applied by hydrothermal process. The study was conducted to investigate the effect of substrate material and ZnO nanostructure on the f-SWCNT surface which embedded on those flexible polymer substrates. Morphological surface of f-SWCNT network and crystal structure of ZnO and f-SWCNT were also observed by scanning electron microscope (SEM) and X-ray diffraction, respectively. The results reveal that f-SWCNT on Si substrate (f-SWCNT/Si) do not have a good response in gas sensing performance. In meanwhile f-SWCNT on PET substrates (f-SWCNT/PET) is more sensitive about 1.6% with 3s in response. Surface structure of f-SWCNTs modified layer by ZnO nanostructure enhanced sensitivity and responsiveness of the sensor with sensitivity reached up 4.1% in 2s response after CO₂ injection. It was observed that the ZnO nanostructured layer enhanced the sensing sensitivity and responsiveness of f-SWCNTs. The ZnO nanowires structure on the surface of f-SWCNTs has successfully improved the performance of CNTs as sensors. The bending treatment of up to 30% can reduce sensor sensitivity and change the configuration and arrangement of the CNT.

ARTICLE HISTORY

Received: 3 Sept 2022

Revised: 4 Oct 2022

Accepted: 11 Oct 2022

KEYWORDS

Gas Sensing Properties

Functionalized SWCNTs

Flexible Substrate

INTRODUCTION

A gas detection devices have been crafted and developed in recent years. This is a preventative stage and effort to save earth from environmental problems [1]–[4]. Carbon dioxide [5]; nitrogen dioxide [6]–[8] and gases of volatile organic compounds such as acetone [9], [10]; ammonia [2], [11], [12] as case studies of dangerous gases are progressively investigated. Reduced graphene oxide [6]; graphene oxide [13]; graphene [2], CNTs, both carbon nanotubes of singlewalled CNTs (SWCNTs) and multiwalled CNTs (MWCNTs), are worthy to be used as gas detection materials because of high surface area for adsorbing molecular gases [14]. Gas molecules and other chemicals on the CNT surface can either donate or accept electrons, resulting in an alteration of the overall conductivity. Such properties make CNTs ideal for nanoscale gas sensing materials.

Carbon nanotubes (CNTs)-based composites have attracted significant research interest in recent years, owing to their important applications which are potentially combined with metals [15], metal oxides, ceramics [11], [16] and conductive polymers such as polyaniline (PANi) [2], [17], poly(α -methylstyrene) (PMS) [9], poly(vinylpyrrolidone) (PVP) [18], and polyethylene terephthalate (PET) [19]. The effect of CNT nanocomposite on electrical conductivity and sensitivity to gas sensing have been investigated [20]–[23]. Metal or metal oxide modification on the CNT surface as hybrid nanocomposites have received a great deal of attention for gas-sensing application due to higher sensitivity over a wide range of gas concentrations at room temperature compared to only using CNTs.

Various substrate materials have been developed such as polyimide substrate for CO₂ and NO₂ gas [14], [24], [25], poly(aniline-co-o-toluidine) substrate for hexavalent chromium gas [26], glass substrate for NH₃, CO₂ and NO₂ gas [5], [23], [27], FET substrate for N₂ and NO₂ sensor [20], Si/SiO₂ substrate for a NO₂ [6], silicon porous substrate for NO₂ gas [28], [29], Quartz substrate and Au IDE for CH₄ gas [16], alumina substrate for H₂S gas [30], PANi substrate for a NH₃ and LPG sensor [11], [17] have been developed. Flexible substrate for standing its active elements offer an advantage in resulting in flexibility of implementation and application avoiding performance deformation.

In this research, we used a metal oxide semiconductor. Zinc oxide (ZnO) is considered as the promising resistive-type gas sensing material where the various ZnO hierarchical structures which possess high surface areas and less aggregation, as well as their corresponding gas sensing performances. ZnO deposition on the surface of f-SWCNT acts as a good gas sensing hybrid material which is still limited to be studied. In addition, the use of very cheap flexible substrate materials provides added value for better performance and ease of implementation on sensors. In this current research, we compared

a sensing property of CNTs embedded in two flexible substrate materials i.e., silicon (Si) rubber film and waste plastic of polyethylene terephthalate (PET). The aim of this work is to investigate the gas sensing performance of f-SWCNTs-based sensors, ZnO/ f-SWCNT hybrid sensor and bending effect on the sensing performance. Evaluation of stability and flexibility as well as response recovery times of the sensors were also investigated in this study. We compared between individual f-SWCNT layer sensor and ZnO-modified f-SWCNT hybrid sensor. We applied f-SWCNT layer on the substrates by spray coating and dip coating techniques for Si and PET substrates respectively and then compared. Scanning electron microscope (SEM) and X-Ray Diffraction was used to study morphological surface and the structure of sensor

EXPERIMENTAL METHOD

Materials

Sodium dodecyl sulfate (SDS); *hexamethylene tetramine* (HMT); *zinc acetate dihydrate* (ZAD); *zinc nitrate hexahydrate* (ZAH) was commercially purchased from Sigma Aldrich Co. *Sodium hydroxide* (NaOH) was obtained from Merck. *Typol* was obtained from Bratachem. *Functionalized single-walled carbon nanotubes* (f-SWCNTs) were obtained from Chengdu Organic Chemicals Co., Ltd, *Polyethylene terephthalate* (PET) film and *silicon* rubber sheet (Si) were purchased as commercial substrate available in the marketplace.

CNT's solution preparation

CNT dispersed solution was prepared by adding 20 mg of f-SWCNT in 30 mL DI water containing 100 mg SDS and then sonicated for 1 h sonication.

Hydrophilic surface treatment of substrate materials

Prior to CNT deposition, surface treatment of substrate materials is required. PET film in dimension of 6x2 cm² was subjected to a series of treatment i.e., washing with DI water containing 1% v/v typol under sonication for 10 min, rinsed in water and dried in a 45°C oven. Subsequently the sample was rinsed with 3M NaOH for 1 h in oven at 60°C, then rinsed with water until the pH was neutral. Silicon rubber film in 4x2 cm² dimension was proceed using a simple treatment i.e., cleaning in ethanol, washing in DI water and finally dried at 60°C in oven, respectively.

Fabrication of CNT film on Si and PET substrate materials by coating techniques

Two coating techniques i.e., dip coating and spray coating were used to deposit CNT film on two substrate materials. Waste plastic of PET film used as CNT template was proceed by dip coating techniques. The controlled parameters were dip speed 2 mm/s, dip time 120 s, and elevated speed 0.2 mm/s. Dip coating process of PET film was cycled for 15 up to 20 times into CNT solution then completely dried in oven. In meanwhile, Si films used as template of CNT film was deposited by spray brush coating. The substrate was then heated on a hotplate at 90°C for a few minutes and then annealed at 90°C for 1 h.

ZnO metal oxide coating on the CNT template by hydrothermal process

Seeding solution was prepared by dissolving a 0.2M ZAD solution in DI water. The solution was ultrasonically sprayed on the surface of CNT film and annealed for 1 h at 90°C. Then, the growth of ZnO nanostructures on the surface of substrates was carried out by immersing in 15 mL of a mixed solution of 0.05 M ZNH and 0.05 M HMT at an angle of 45°, at 100°C for 6 h by hydrothermal process. After the process, the samples were washed with DI water to remove a number of white particles on the surface. The resulting ZnO nanostructures were finally dried at 50°C for 12 h [31].

Surface morphology and structure

Scanning electron microscopy (SEM) was used to observe CNT film composites surface. Prior to SEM observation, conductive sample was provided by sputtering gold and observed in optaiming voltage 20.0 kV. Crystal structure of all samples was characterized by X-ray powder diffraction (XRD) Rigaku with Cu K α radiation ($\lambda = 1.5418$) with scanning rate 5°/min in the diffraction range of $2\theta=10-90^\circ$.

Measurement of gas sensing properties

CO₂ gas sensing measurement of CNT nanocomposite was performed in a closed chamber which recorded using a Kiethley Sourcemer 2450 interfaced with computer at room temperature as schematic illustrated in Figure 1a. CO₂ gas were injected into the chamber at a gas flow of 1000 cm³ min⁻¹. CO₂ gas sensitivity can be measured as the normalized resistance change by:

$$R = \frac{(R_g - R_0)}{R_0} \times 100\% \quad (1)$$

where R_g is resistance value after gas exposure and R₀ is resistance value at the initial stage. Prior to sensing test, CO₂ gas purge into the chamber for 15 min to set room condition

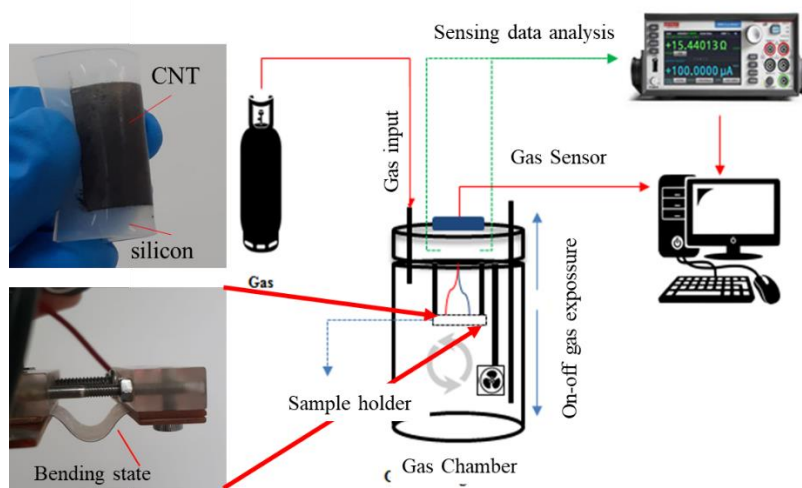


Figure 1. Gas sensing setup of the CNT-based thin film

RESULTS AND DISCUSSION

Morphological Surface of CNT nanocomposites films

Figure 2a shows the smooth surface morphology of the f-SWCNT-deposited silicon. White patches on the Si surface were observed on the silicon substrate. This probably stems from the agglomeration of CNTs trapped beneath the Si surface as it softened at 90 °C during the heating process. Meanwhile, Figure 2c shows the morphology of the CNT tissue which is clearly visible on the PET surface that has been hydrolyzed. The CNT tube network is more clearly embedded in the PET surface. The floated material observed on the surface was thought to be particulate surfactant residue. We deposited ZnO onto f-SWCNT films embedded in 2 substrate materials by a hydrothermal process. The hydrothermal process forms two different ZnO structures on different substrate materials. The flower structure of ZnO with an average size of 536 nm was observed on the Si substrate (Figure 2b) and the nanowire structure of ZnO (Fig. 2d) was observed on the PET substrate with a diameter of 86 nm which is smaller than the flower structure of ZnO on the Si surface. Different substrate materials give different seed layers which affect the structural properties of ZnO or even give different gas sensing properties [32]–[34].

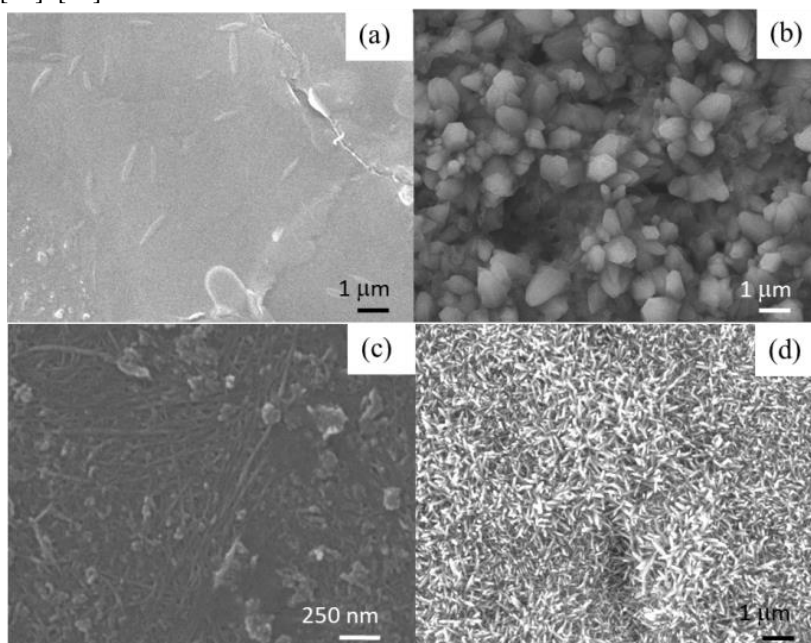


Figure 2. SEM Surface Morphology of SWCNT on top view (a) f-SWCNT/Si; (b) ZnO/f-SWCNT/Si; (c) f-SWCNT/PET; and (d) ZnO/f-SWCNT/PET.

ZnO nanowires on PET substrate have a size distribution of about 0.04–0.14 μm smaller than that the flowery structure on Si substrate with a size of 0.2–1.2 μm (Figure 3). Small crystal sizes have a large specific surface area [35]. Smaller particle sizes such as ZnO nanowires are useful for more effective gas adsorption on surfaces which may be closely related to sensor response and sensitivity.

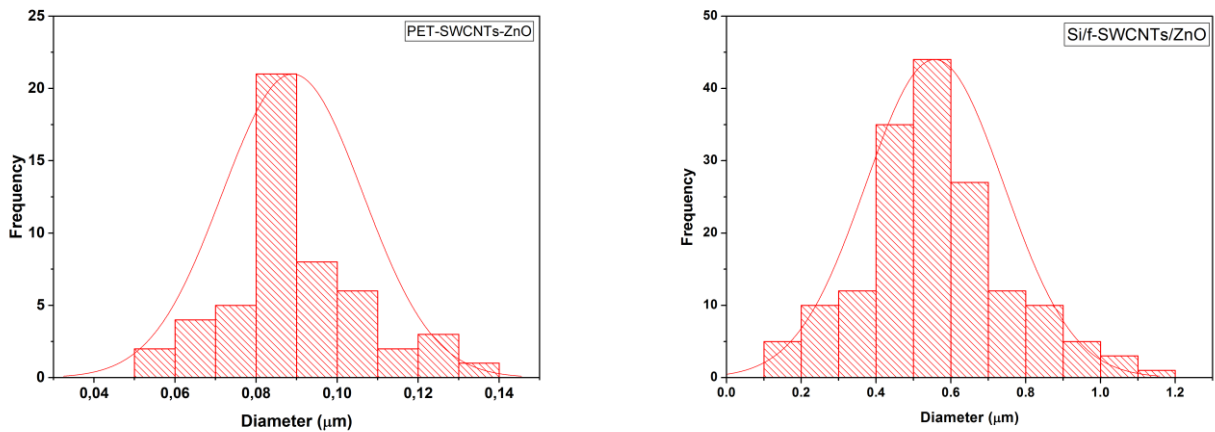


Figure 3. Size Distribution of ZnO on Si (a) and PET (b) Substrate.

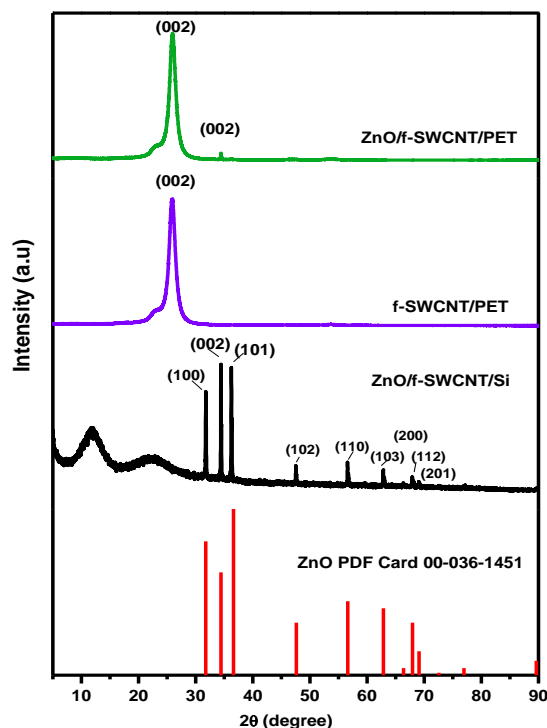


Figure 4. XRD for CNTs and ZnO/CNTs films.

Structural Analysis of ZnO by X-Ray Diffraction

Figure 4 shows X-ray diffraction graphs of naked f-SWCNTs and ZnO/f-SWCNTs deposited on two substrate materials of Si and PET. The pure ZnO nanostructures show a polycrystalline form, according to the standard card 000-036-1451. The diffraction peaks of ZnO/f-SWCNTs/Si appear at $2\theta = 31.77^\circ, 34.42^\circ, 36.25^\circ, 47.54^\circ, 56.60^\circ, 62.86^\circ, 67.96^\circ$ which are associated with (100), (002), (101), (102), (110), (103), and (112) crystal lattice planes of the ZnO hexagonal wurtzite structure, respectively. The amorphous peaks of ZnO/f-SWCNT/Si at a diffraction angle of less than $2\theta_0$ can be confirmed to be related to the polymeric structure of the silicon substrate. The most intense peak appears at $2\theta = 34.42^\circ$ as (002) ZnO diffraction plane which also appears at ZnO/f-SWCNT/PET with very low intensity. Meanwhile, the sharp peak intensity of the diffraction plane (002) at $2\theta = \sim 24^\circ$ corresponds to the CNT hexagonal graphite structure. The diffraction grating (002) of the hexagonal graphite structure was clearly identified as a sharp peak intensity in the f-SWCNT/PET and ZnO/f-SWCNT/PET samples. X-ray diffraction of ZnO/f-SWCNTs/PET films showed a low peak intensity of ZnO at $2\theta = 34.42^\circ$ which was associated with (002) hexagonal wurtzite structure according to class C6v4 (Schoenflies notation) and space group P63mc (Herman-Mauguin notation) [36].

Gas Sensing Properties of CNT

We investigated the sensing properties of the f-SWCNT-based sensor and compared it with the ZnO/f-SWCNT-based nanohybrid sensor on Si and PET substrate materials. Sensors have different responses on different substrates. The

characteristic noise of f-SWCNT/Si indicates that the sensor does not respond well to CO₂ gas as an indication that CO₂ gas is not well adsorbed by the f-SWCNT surface and there is an inhibition of charge transfer on the surface. The CNT tube trapped under the Si surface causes the closure of the active CNT groups, resulting in gas adsorption and low electron density. The active group f-SWCNT acts as a charge transfer agent between CO₂-CNT. The active group trapped on the surface of Si substrate causes sensor to be less responsive and less sensitive, as shown in Figure 5a.

Meanwhile, the current response of the f-SWCNTs/PET-based sensor increased rapidly after the gas is injected and then stabilized. When the CO₂ gas in the chamber is disturbed by air injection, the f-SWCNT/PET sensor current rapidly decreases and returns to its initial state (Figure 5b). CO₂ gas emits electrons, which become trapped on the surface and form a thick layer of spatial charge, increasing the potential barrier. Changes in current response indicate changes in electron density on the surface of the f-SWCNT. The active group of f-SWCNT is important in gas adsorption, which is thought to be a medium for charge transfer between CO₂ molecules and f-SWCNT. The sensor's sensitivity is around 1.63%. Figure 5c,d show a hybrid ZnO/f-SWCNT structure with dynamic responses and excellent sensing properties for CO₂ gas detection. The sensitivity of ZnO/f-SWCNT/PET increased to 4.1% with a response time of 2 seconds (Figure 5d). The current response of ZnO/CNTs is doubled when compared to naked f-SWCNTs, indicating that the hybrid structure of ZnO-CNT forms a p-n junction, where ZnO is an n-type semiconductor and carbon nanotubes (CNTs) are p-type semiconductors. In such a case, the resistive gas sensor may be used. This demonstrates that improving gas sensing properties necessitates the use of both p-type and n-type materials [37].

The sensing mechanism is based on the analyte's interaction with the n-type of ionic oxygen to be oxidized, which then releases electrons back into the ZnO conduction band as a result of exposure to reducing gases such as H₂S, H₂, and C₂H₅OH. Furthermore, this species is exposed to oxidizing gases such as SO₂, NO_x, and O₃, which exhibit a decrease in the density of free charge carriers. When the oxidizing gas is absorbed on the surface of ZnO, it captures electrons, resulting in an increase in resistance [38], [39]. ZnO site in the crystal defect of CNT due to oxidation process. Active groups, OH, COOH, CO on the CNT surface play important role to generate the good interaction with another molecules.

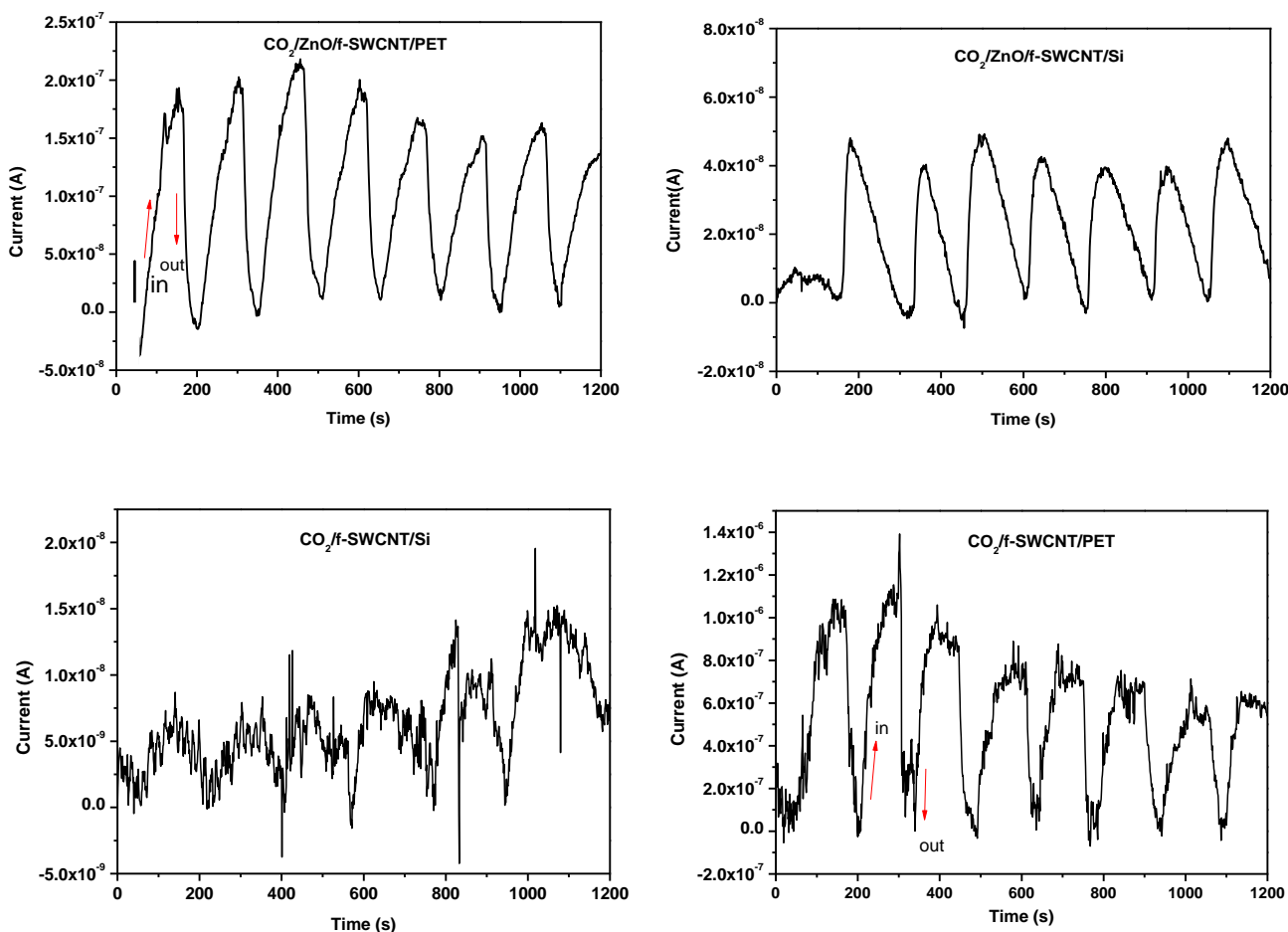


Figure 5. Sensing Properties of f-SWCNT and ZnO/f-SWCNTs on PET and Si film substrate for CO₂ gas

SWCNTs are doped by the electron-rich ZnO which enhanced electron density of the sensor. for f-SWCNT/PET and ZnO/f-SWCNTs/PET, respectively. Current response of ZnO/f-SWCNTs/PET increases in CO₂ environment because a smaller number of carriers trapped in ZnO boundaries and more electrons are liberated (Figure 6). Electron have an easier transport in ZnO/f-SWCNT/PET sensor than CNT/PET indicating ZnO/CNTs film is a more efficient CO₂ sensor than

CNT film. CNT-based gas sensors have an active surface which can transfer charge between CNTs to gas molecules upon their interaction. Such case induces changes in the electrical conductivity of the CNTs. CO₂ molecule adsorption by CNT surfaces provide an charge transfer between gas molecules and CNT.

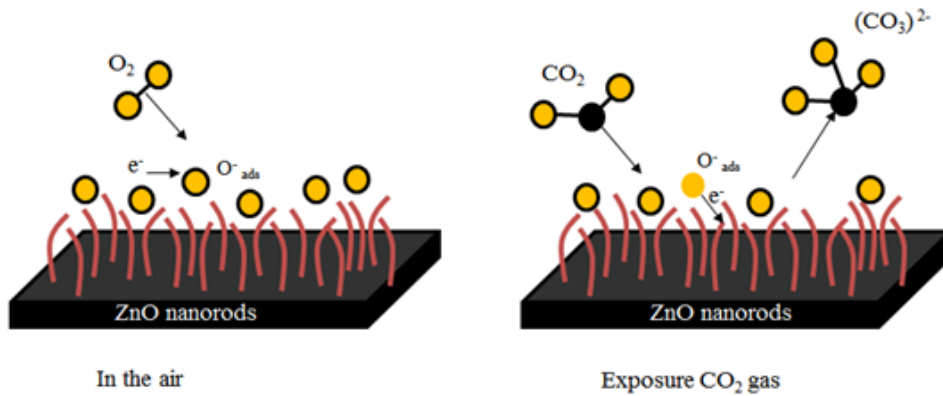


Figure 6. Illustration Figure of CO₂ Gas Adsorption – Desorption

From the above analysis, we selected ZnO/f-SWCNT/PET for further performance test. We bent the sample separately about 19% and 30% of the original length (18.85 mm) during on-off CO₂ gas exposure (Figure 7). In the bending treatment, our sensor still showed good response to CO₂ gas. Meanwhile, bending test of ZnO/f-SWCNT/PET about 19% and 30% on CO₂ gas demonstrate constantly its responsiveness, with response time of 7s and 9s and sensitivity of 1.8 and 1.34 %, respectively

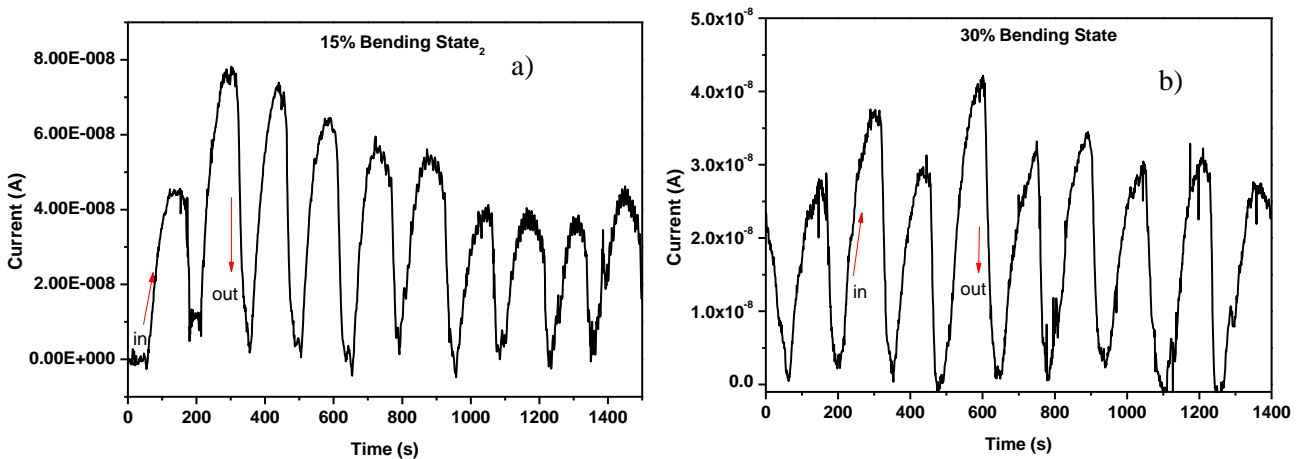


Figure 7. Sensing Properties of ZnO/f-SWCNT/PET under bending treatment of 19% (a) and 30% (b) and on-off CO₂ Gas Exposure.

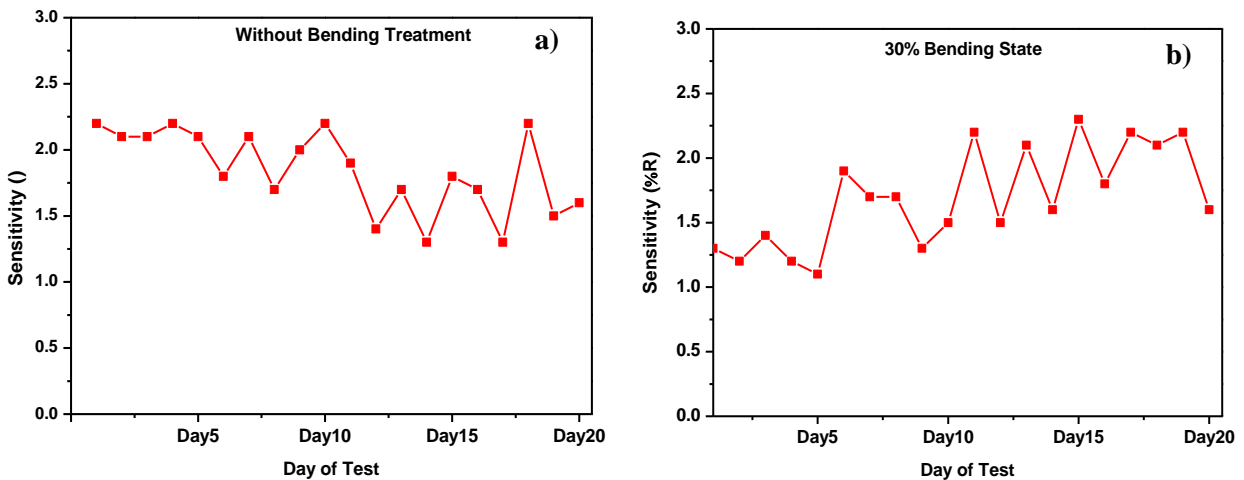


Figure 8. Sensing Stability Properties test of ZnO/f-SWCNT/PET with and without bending treatment

There is a decrease in sensor response compared to the initial state. Bending level determines configuration of CNT element and causes differences in the effectiveness of gas adsorption. Therefore, the configuration and network of CNT elements causes changes in the overall electrical conductivity of the sensor as shown in this current research which have been comprehensively studied by Yudianti, et al on CNT-based wearable sensors [40].

Further investigation of the stability of the ZnO/f-SWCNT/PET response was carried out on samples with and without bending treatment. The investigations were carried out for 20 consecutive days with 30% bending (Figure 8) and compared with baseline. Our sensor still showed a response when the 30% bending treatment was carried out for 20 days. On average they have the same performance sensitivity, did not show significant changes or experience excessive performance degradation. However, in the initial state (up to day 5), the bending treatment by 30% experienced a reduction in sensitivity as shown in the low sensitivity period showing a low current response. After that period, the sensor shows a slightly increased response and tends to reach a stable state. Finally, they did not have a significant difference in the stability. Indeed, we used no-bending sample which have a change in performance compared with the previous sample. CNT-based gas sensor required heating treatment to recovery its surface from gas molecule. However, the whole experiment work described the importance ZnO/f-SWCNT hybrid structure build p-n junction nanostructure for gas detection.

CONCLUSION

In this research paper, we have demonstrated a simple and efficient method for fabricating a SWCNT-based gas sensor that exhibited outstanding sensing properties as a gas sensor. The hybrid structure of ZnO/f-SWCNT exhibited excellent sensing properties for CO₂ gas detection with a sensitivity of 4.1% and a response time of 2 seconds. The decorated ZnO nanowires structure on the f-SCWNT surface has successfully improved the sensing properties of the sensor. The bending treatments of 19% and 30% have reduced their sensitivity to 1.8% and 1.3%, respectively. The bending treatment caused a decrease in sensor sensitivity as an indication of a change in the configuration and network of the CNT. However, our sensors have slight good stability performance for 20 days.

ACKNOWLEDMENT

We acknowledge to National Research and Innovation Agency (BRIN) for research funding and facilities. We thank Surip Kartolo for his technical assistance in setting up the gas chamber.

REFERENCES

- [1] R. Ghanbari, R. Safaiee, M. H. Sheikhi, and M. M. Golshan, "Graphene Decorated with Silver Nanoparticles as a Low- Temperature Methane Gas Sensor," *ACS Appl. Mater. Interfaces*, vol. 11, pp. 21795–21806, 2019.
- [2] F. A. Tabar, A. Nikfarjam, N. Tavakoli, J. N. Gavgani, and M. Mahyari, "Chemical-resistant ammonia sensor based on polyaniline / CuO nanoparticles supported on three-dimensional nitrogen-doped graphene-based framework nanocomposites," *Microchim Acta*, pp. 1–13, 2020.
- [3] C. Wang, Y. Li, F. Gong, Y. Zhang, and S. Fang, "Advances in doped ZnO nanostructures for gas sensor," *Chem. Rec.*, vol. 20, pp. 1–16, 2020.
- [4] U. Kumar and B. C. Yadav, "Synthesis of carbon nanotubes by direct liquid injection chemical vapor deposition method and its relevance for developing an ultra-sensitive room temperature based CO₂ sensor," *J. Taiwan Inst. Chem. Eng.*, vol. 96, no. 2, pp. 652–663, 2019.
- [5] R. Saad *et al.*, "Fabrication of ZnO/CNTs for Application in CO₂ Sensor at Room Temperature," *Nanomaterials*, vol. 11, no. 11, p. 3087, Nov. 2021.
- [6] N. Lim, J. S. Lee, and Y. T. Byun, "Negatively-doped single-walled carbon nanotubes decorated with carbon dots for highly selective NO₂ detection," *Nanomaterials*, vol. 10, no. 12, pp. 1–11, 2020.
- [7] Y. Kang, F. Yu, L. Zhang, W. Wang, L. Chen, and Y. Li, "Review of ZnO-based nanomaterials in gas sensors," *Solid State Ionics*, vol. 360, no. December 2020, p. 115544, 2021.
- [8] N. M. Al-Makram and W. R. Saleh, "Functionalized multi-walled carbon nanotubes network sensor for NO₂gas detection at room temperature," *AIP Conf. Proc.*, vol. 2290, no. 2, 2020.
- [9] J. C. Chiou and C. C. Wu, "A wearable and wireless gas-sensing system using flexible polymer/multi-walled carbon nanotube composite Films," *Polymers (Basel)*, vol. 9, no. 9, 2017.
- [10] S.-J. Young *et al.*, "Multi-Walled Carbon Nanotubes Decorated with Silver Nanoparticles for Acetone Gas Sensing at Room Temperature," *J. Electrochem. Soc.*, vol. 167, no. 16, pp. 1–9, 2020.

- [11] N. Ansari *et al.*, “Trace level toxic ammonia gas sensing of single-walled carbon nanotubes wrapped polyaniline nanofibers,” *J. Appl. Phys.*, vol. 127, no. 4, 2020.
- [12] L. Xue, W. Wang, Y. Guo, G. Liu, and P. Wan, “Sensors and Actuators B : Chemical Flexible polyaniline / carbon nanotube nanocomposite film-based electronic gas sensors,” *Sensors Actuators B. Chem.*, vol. 244, pp. 47–53, 2017.
- [13] H. Wang *et al.*, “Graphene-Like Porous ZnO / Graphene Oxide Nanosheets for High-Performance Acetone Vapor Detection,” *Molecules*, vol. 24, p. 522, 2019.
- [14] M. Han, S. Jung, Y. Lee, D. Jung, and S. Kong, “PEI-functionalized carbon nanotube thin film sensor for CO₂ gas detection at room temperature,” *Micromachines*, vol. 12, no. 9, pp. 1–11, 2021.
- [15] R. Yudianti, H. Onggo, I. Riyati, and S. Rman, “Role of Catalytic Synthesis on Growth and Distribution of Platinum Nanoparticle on Carbon Nanotube Surface,” *Nanosci. Nanotechnol.*, vol. 2, no. 6, pp. 171–177, Jan. 2013.
- [16] N. Janudin *et al.*, “Low Cost and Room Temperature Methane Detection using Multi Walled-Carbon Nanotubes Functionalized with Octadecanol,” *J. Def. Sci. Eng. adn Technol.*, vol. 1, no. 2, pp. 65–75, 2018.
- [17] H. Albaris and G. Karuppasamy, “Fabrication of room temperature liquid petroleum gas sensor based on PANi–CNT–V₂O₅ hybrid nanocomposite,” *Appl. Nanosci.*, vol. 9, no. 8, pp. 1719–1729, 2019.
- [18] Y. H. Ngo *et al.*, “Chemically Enhanced Polymer-Coated Carbon Nanotube Electronic Gas Sensor for Isopropyl Alcohol Detection,” *ACS Omega*, vol. 3, no. 6, pp. 6230–6236, 2018.
- [19] C. Fang *et al.*, “Effect of multi-walled carbon nanotubes on the physical properties and crystallisation of recycled PET/TPU composites,” *RSC Adv.*, vol. 8, no. 16, pp. 8920–8928, 2018.
- [20] S. Forel, L. Sacco, A. Castan, I. Florea, and C. S. Cojocaru, “Simple and rapid gas sensing using a single-walled carbon nanotube field-effect transistor-based logic inverter,” *Nanoscale Adv.*, vol. 3, no. 6, pp. 1582–1587, 2021.
- [21] M. Shoostari, A. Salehi, and S. Vollebregt, “Effect of Humidity on Gas Sensing Performance of Carbon Nanotube Gas Sensors Operated at Room Temperature,” *IEEE Sens. J.*, vol. 21, no. 5, pp. 5763–5770, 2021.
- [22] S. I. Hwang *et al.*, “Breath Acetone Sensing Based on Single-Walled Carbon Nanotube-Titanium Dioxide Hybrids Enabled by a Custom-Built Dehumidifier,” *ACS Sensors*, vol. 6, no. 3, pp. 871–880, 2021.
- [23] W. Xuan Du *et al.*, “Highly sensitive single-walled carbon nanotube/polypyrrole/phenylalanine core-shell nanorods for ammonia gas sensing,” *J. Mater. Chem. C*, vol. 8, no. 44, pp. 15609–15615, 2020.
- [24] B. Liu *et al.*, “A flexible NO₂ gas sensor based on polypyrrole/nitrogen-doped multiwall carbon nanotube operating at room temperature,” *Sensors Actuators, B Chem.*, vol. 295, no. 2, pp. 86–92, 2019.
- [25] J. Chiou, C. Wu, and T. Lin, “Sensitivity Enhancement of Acetone Gas Sensor using Polyethylene Glycol/Multi-Walled Carbon Nanotubes Composite Sensing Film with Thermal Treatment,” *Polymers (Basel)*, vol. 11, no. 3, p. 423, 2019.
- [26] M. A. Hussein *et al.*, “Electrochemical sensor-based gold nanoparticle / poly (aniline-co-o-toluidine)/ graphene oxide nanocomposite modified electrode for hexavalent chromium detection : a real test sample detection : a real test sample,” *Polym. Technol. Mater.*, vol. 00, no. 00, pp. 1–14, 2019.
- [27] S. Barthwal and N. B. Singh, “ScienceDirect ZnO-SWCNT Nanocomposite as NO₂ gas sensor,” *Mater. Today Proc.*, vol. 5, no. 7, pp. 15439–15444, 2018.
- [28] S. K. Abbas and A. N. Naje, “Functionalized carbon nanotubes on porous silicon for sensing application,” *J. Nano- Electron. Phys.*, vol. 11, no. 5, 2019.
- [29] A. N. Naje and W. K. Mahmood, “Sensitivity Performance of Single Wall Carbon Nanotubes Gas Sensor on Silicon and Porous Silicon,” *IOP Conf. Ser. Mater. Sci. Eng.*, vol. 454, no. 1, 2018.
- [30] J. H. Bang *et al.*, “Decoration of multi-walled carbon nanotubes with CuO/Cu₂O nanoparticles for selective sensing of H₂S gas,” *Sensors Actuators, B Chem.*, vol. 344, no. January 2020, p. 130176, 2021.
- [31] A. Syampurwadi, I. Primadona, V. Fauzia, and Isaeni, “Photoreduction of palladium nanoparticles on ZnO nanorods for enhancing photocatalytic decolorization of methylene blue,” *IOP Conf. Ser. Earth Environ. Sci.*, vol. 483, no. 1, p. 012042, Mar. 2020.
- [32] Z. H. Azmi, S. N. Mohd Aris, S. Abubakar, S. Sagadevan, R. Siburian, and S. Paiman, “Effect of Seed Layer on the Growth of Zinc Oxide Nanowires by Chemical Bath Deposition Method,” *Coatings*, vol. 12, no. 4, 2022.
- [33] N. Rosli, M. M. Halim, M. R. Hashim, W. Maryam, M. F. M. Rusdi, and A. R. Muhammad, “Effect of the Seeding Thickness on the Growth of ZnO Nanorods prepared by CBD,” *IOP Conf. Ser. Mater. Sci. Eng.*, vol. 854, no. 1,

2020.

- [34] C. Li, G. Fang, J. Li, L. Ai, B. Dong, and X. Zhao, "Effect of seed layer on structural properties of ZnO nanorod arrays grown by vapor-phase transport," *J. Phys. Chem. C*, vol. 112, no. 4, pp. 990–995, 2008.
- [35] R. Maheswaran and B. P. Shanmugavel, "A Critical Review of the Role of Carbon Nanotubes in the Progress of Next-Generation Electronic Applications," *J. Electron. Mater.*, vol. 51, no. 6, pp. 2786–2800, Jun. 2022.
- [36] A. Galdámez-Martínez, G. Santana, F. Güell, P. R. Martínez-Alanis, and A. Dutt, "Photoluminescence of ZnO Nanowires: A Review," *Nanomaterials*, vol. 10, no. 5, p. 857, Apr. 2020.
- [37] T. Sujitno, T. Atmono, Sayono, and L. Susita, "LAPISAN TIPIS ZnO SUSUNAN LARIK SEBAGAI SENSOR GAS," *Ganendra*, vol. IX, no. 2, pp. 11–20, 2006.
- [38] R. Kumar, O. Al DOssary, G. Kumar, and A. Umar, "Zinc Oxide Nanostructures for NO₂ Gas – Sensor Applications : A Review," *Nano-Micro Lett.*, vol. 7, no. 2, pp. 97–120, 2015.
- [39] M. A. Franco, P. P. Conti, R. S. Andre, and D. S. Correa, "A review on chemiresistive ZnO gas sensors," *Sensors and Actuators Reports*, vol. 4, no. March, p. 100100, 2022.
- [40] R. T. Yulianti *et al.*, "Highly Stretchable and Sensitive Single-Walled Carbon Nanotube-Based Sensor Decorated on a Polyether Ester Urethane Substrate by a Low Hydrothermal Process," *ACS Omega*, vol. 6, no. 50, pp. 34866–34875, Dec. 2021.



Copyright © 2022 Jusami | Indonesian Journal of Material Science. This article is open access article distributed under the terms and conditions of the [Creative Commons Attribution-NonCommercial-ShareAlike 4.0 International License \(CC BY-NC-SA 4.0\)](https://creativecommons.org/licenses/by-nc-sa/4.0/)